

A Pharmacodynamic Turnover Model Capturing Asymmetric Circadian Baselines of Body Temperature, Heart Rate and Blood Pressure in Rats: Challenges in Terms of Tolerance and Animal-handling Effects

Björn Sällström,¹ Sandra A. G. Visser,¹ Tomas Forsberg,²
Lambertus A. Peletier,^{3,4} Ann-Christine Ericson,²
and Johan Gabriëlsson^{5,6}

Received August 1, 2005—Final September 26, 2005

This study presents development and behaviour of a feedback turnover model that mimics asymmetric circadian oscillations of body temperature, blood pressure and heart rate in rats. The study also includes an application to drug-induced hypothermia, tolerance and handling effects. Data were collected in normotensive Sprague-Dawley rats, housed at 25 °C with a 12:12 hr light:dark cycle (light on at 06:00 am) and with free access of food and water. The model consisted of two intertwined parallel compartments which captured a free-running rhythm with a period close to but not exactly 24 hrs. The free-running rhythm was synchronised to exactly 24 hrs by the environmental timekeeper (12:12 hr light on/off cycle) in experimental settings. The baseline model was fitted to a standardised 24-hr period derived from mean data of six animals over a period of nine consecutive days. The first-order rate constants related to the turnover of the baseline temperature, α and β , were 0.026 min^{-1} ($\pm 5\%$) and 0.0037 min^{-1} ($\pm 3\%$). The α and β parameters are approximately $2/\text{transition time between day and night}$ and $2/\text{night time}$, respectively. The day:night timekeeper $g(t)$, reference point T_{ref} and amplitude were $0.053(\pm 2\%)$, $37.3(\pm 0.02\%)$ and 3.3% ($\pm 2\%$), respectively. Simulations with the baseline model revealed stable oscillations (free-running rhythm)

¹PKPD section, B231, Local Discovery Research Area CNS & Pain Control, AstraZeneca R&D Södertälje, SE-151 85 Södertälje, Sweden.

²Department of General Pharmacology, Local Discovery Research Area CNS & Pain Control, AstraZeneca R&D Södertälje, SE-151 85 Södertälje, Sweden.

³Mathematical Institute, Leiden University, Niels Bohrweg 1, P.O. Box 9512, 2300 RA, Leiden, The Netherlands.

⁴Centrum voor Wiskunde en Informatica, P.O. Box 94079, 1090 GB Amsterdam, The Netherlands.

⁵DMPK & Bioanalytical Chemistry, AP305, AstraZeneca R&D Mölndal, SE-431 83 Mölndal, Sweden.

⁶To whom correspondence should be addressed. E-mail: Johan.Gabriëlsson@AstraZeneca.com

in the absence of the timekeeper. This temperature–time profile was then symmetric and had a smaller amplitude, with a slightly shorter period and less pronounced temperature shift as compared to the profile in the presence of an external Timekeeper. Fitting the model to 96 hr mean profiles of blood pressure and heart rate from 10 control animals demonstrated the usefulness of the model. Simulations of the integrated temperature model succeeded in mimicking other modes of administration such as oral dosing.

KEY WORDS: pharmacodynamics; turnover model; mathematical model; set-point; free-running rhythm; circadian rhythm; oscillating model; chronobiology; Zeitgeber.

INTRODUCTION

Chronobiological rhythms (e.g., circadian) of diverse physiological variables such as cardiovascular changes, endocrinological systems (e.g., insulin, oestradiol, follicle-stimulating hormone, growth hormone, prolactin), locomotor activity and body temperature are common phenomena. The intrinsic behaviour of a biorhythm in the absence of an external timekeeper is supported by previously published experimental data such as locomotor activity, body temperature and plasma corticosterone (1,2). There are substantial challenges in obtaining a biorhythm model for these responses, because patterns are often asymmetric with different day/night time courses and are also entrained by external timekeepers such as the 12:12 light/dark cycle in laboratory settings.

From a pharmacokinetic–dynamic reasoning in general and a drug discovery perspective in particular, a correct description of the normal baseline biorhythms is of importance in order to avoid biased or imprecise results and is used primarily for optimal design of *in vivo* pharmacology studies. Some methods have recently been used to describe biorhythms, most of which are based on trigonometric functions such as a single cosine function or Fourier series (3,4). Others have used self-oscillating differential equations for glucose/insulin turnover. For our purposes of using body temperature, blood pressure or heart rate in a safety pharmacological setting, there are no straightforward methods of capturing free-running biorhythms or asymmetric circadian profiles, tolerance development to drug effects or even animal-handling effects. This is, nevertheless, of considerable importance in order to separate not only genuine drug effects from biorhythms, but also other disturbances such as handling effects during administration of a test compound or disturbances due to animal care (e.g., changing water bottles).

Accordingly, the aims of this report are to propose, for our purposes in *in vivo* pharmacology, a turnover model of biorhythms and to challenge the model by additional experimental data and model simulations.

A Pharmacodynamic Turnover Model

The additional experiments included data derived from 5 days' constant exposure to a new analgesic compound for which tolerance to body temperature was observed. Also, a simple function for animal-handling was introduced. Finally, model simulations were performed in order to mimic the impact of other modes of administration of the test compound for comparisons with experimental data.

MATERIALS AND METHODS

Animals

Male Sprague-Dawley rats (Supplier B&K Scanbur AB, Sollentuna, Sweden) that had been acclimatised for at least 5 days were used for the *in vivo* studies. During the experiments, the rats were housed individually in transparent cages with wood shavings as bedding and with free access to food (Lactamin, Stockholm, Sweden) and tap water under the following environmental conditions: temp: 18–22 °C; humidity: 40–60%; ventilation: 15–20 air changes per hour; artificial illumination: 12 hr light/12 hr dark (lights on at 6 am). All *in vivo* body temperature data and blood samples were collected at the Department of General Pharmacology, AstraZeneca R&D Södertälje, Sweden.

The baseline body temperature data were recorded in six control animals for nine consecutive days (5 days prior to and 4 days during continuous subcutaneous infusion). Heart rate and blood pressure were recorded in 10 untreated animals for 4 consecutive days.

Permission was obtained from the Animal Ethics Committee, Stockholm South, Sweden.

Physiological Measurement

Body temperature, blood pressure and heart rate were continuously monitored for 5–7 days in freely moving rats using a telemetric system (PhysioTel Telemetry system, DSI). A transmitter (Physiotel implant TL11M2-C50PXT system, Data Sciences, St. Paul, Minn., USA) was surgically implanted into the peritoneal cavity of each rat at least 3 days prior to the start of measurement. The cage was placed on a corresponding receiver plate (PhysioTel™ Receiver models, RLA2000, RLA 1020 and RPC-1, Data Sciences, St. Paul, Minn., USA) connected to a computer through a Dataquest Exchange Matrix. Body temperature, heart rate and blood pressure were measured at regular intervals (every 2–60 min) and exported to Microsoft Excel.

Chemicals and Dosing

An experimental alpha receptor agonist (test compound) being developed for the indication pain (AstraZeneca) was given either via either continuous subcutaneous (s.c.) administration or oral administration (gavage). See Table I for experimental design. Test compound solutions were prepared on the day of use. Saline (9 mg/ml, Braun Medical AB, Bromma, Sweden) was used as vehicle.

Alzet[®] osmotic minipumps (Model 2001d, 8 μ l/h) were used for continuous s.c. delivery of the test compound. Three different infusion rates of 25, 100 and 200 $\text{nmol} \cdot \text{kg}^{-1} \cdot \text{h}^{-1}$ were used. The Alzet[®] pumps were preincubated in saline at 37 °C for 3 hr prior to being inserted s.c. At the time of dosing, a small incision was made in the back of the animal and the pump was inserted with the flow modulator pointing away from the incision. The pumps were removed after the 5-day infusion period. The animals were briefly anaesthetised with 5% enflurane during insertion and removal.

Two different oral dosing rates of 500 and 1550 $\text{nmol} \cdot \text{kg}^{-1} \cdot \text{day}^{-1}$ of the test compound were used and the doses were given twice daily at 9 am and 3 pm for 7 days. Vehicle-treated animals were used as controls.

Blood Sampling and Plasma Concentration Analysis

Blood samples were drawn from some animals *via* a tail vein at 24, 96 and 120 hr during the continuous s.c. infusion and at 0.5, 1, 2 and 4 hr on day 7 of oral dosing in order to confirm plasma exposure to test compound. Variability of the assay was below 20% and the concentrations were within the calibration curve. Plasma samples were analysed for the test compound at Bioanalytical Chemistry, AstraZeneca R&D Södertälje, Sweden.

Table I. Dose, Units, Regimen, Duration and Number of Animals

Dose	Units	Regimen	Duration (days)	No. of animals
100*	$\text{nmol} \cdot \text{kg}^{-1} \cdot \text{h}^{-1}$	i.v. injection	acute dosing	3
400*		p.o. gavage	acute dosing	3
25	$\text{nmol} \cdot \text{kg}^{-1} \cdot \text{h}^{-1}$	s.c. Alzet [®]	5	3
100				6
200				3
0	$\text{nmol} \cdot \text{kg}^{-1} \cdot \text{day}^{-1}$	Twice gavage	7	3
500		2 \times 250		6
1550		2 \times 750		5

* Was included for assessment of the pharmacokinetics of test compound in a screening study.

Modelling of Biorhythms

The biorhythm model was designed to describe the normal baselines of body temperature, blood pressure and heart rate in untreated rats. Typical characteristics of this baseline profile are:

- Sharp jumps at the transition from day to night and from night to day
- A low, and slowly increasing response-time course during the day
- A high, and slightly decreasing profile during the night

These features suggest a relaxation oscillation such as described by the classical Van der Pol oscillator (5). Thus, this oscillator was chosen as a starting point of the construction. The effect of night and day was incorporated by adding a forcing term with a 24 hr period, the *Zeitgeber* or time keeper. It was off during the day and on during the night. Such a system would still yield a symmetric baseline profile: the shape of the profile would be the same during night and day time, only reversed. To introduce the required asymmetry into the profile, one of the two differential equations was modified so that at night a stationary point is created in the first quadrant. As a result of this modification, the orbit has the following properties: During the night time, when the time keeper is on, the orbit slowly approaches the stationary point in the first quadrant. During day time, when the time keeper is off, the orbit stays away from the stationary point, which is now located at the origin. This causes the orbit to move faster than at night and yields a significantly increasing baseline profile.

These considerations lead to a biorhythm model, which consists of two coupled turnover equations involving two variables B_1 and B_2 and three parameters: the rate constants α and β and a parameter d which measures the difference between light and dark stimuli (Block 1 in Fig. 1). We have designed the system so that the variable B_1 is related to the physiological variable, such as body temperature, the blood pressure or the heart rate, whose oscillatory behaviour we wish to model. The complementary variable B_2 has no special physiological meaning. This block gives the free-running behaviour of the response.

The differential equations that govern the behaviour of B_1 and B_2 are mathematically expressed as

$$\begin{cases} \frac{dB_1}{dt} = \alpha \cdot (B_1 - B_2) - B_1^3 + g(t) \\ \frac{dB_2}{dt} = \beta \cdot (B_1 - B_2) \end{cases} \quad (1)$$

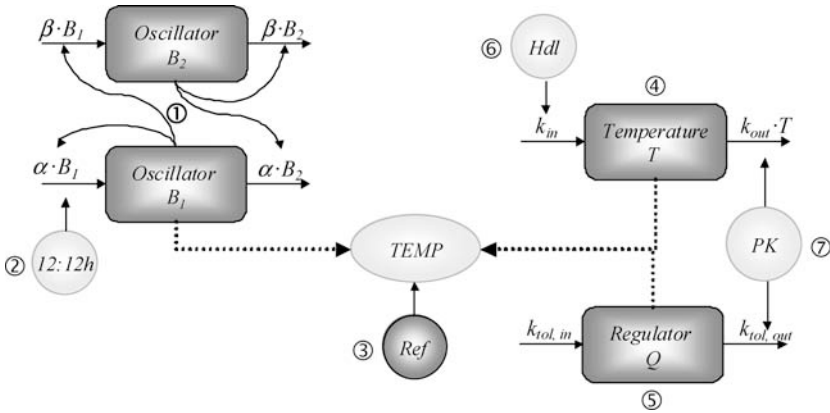


Fig. 1. Schematic illustration of the integrated response (e.g., temperature) model. Block 1 is the free-running turnover model giving the oscillatory behaviour of the baseline. Block 2 is the external 12:12 hr light on:light off cycle. Block 3 is the response function scaling the oscillatory behaviour to actual body temperature. Block 4 represents the turnover of response on which the test compound is acting and Block 5 is the turnover function describing tolerance development. Block 6 is the handling effect acting on the turnover rate of response. Block 7 describes the plasma kinetics of test compound.

where α and β are first-order rate constants (min^{-1}) and the timekeeper $g(t)$ describes the external light conditions (light on/off). The turnover rates (input) for both B_1 and B_2 are governed by B_1 , whereas the loss of both is governed by B_2 . A negative feedback loop is formed by B_2 , in that an increase in B_1 stimulates an increase in B_2 , which is then fed back into B_1 , resulting in an increased loss of B_1 . Any change in B_1 will be *amplified* as an increased loss *via* the term $-B_1^3$. The choice of an exponent of 3 was dictated by the fact that for this value we obtained periodic orbits that fit the data. This model is empirical in the sense that none of α , β , B_1 or B_2 are direct physiological measures. When the Timekeeper $g(t)$ is set equal to zero, then, provided $\alpha > \beta$, this system has a unique stable periodic orbit which attracts orbits starting from arbitrary nonzero initial data $(B_1(0), B_2(0))$. The Timekeeper $g(t)$, which we have modeled as a square wave function,

$$g(t) = \begin{cases} 0 & 6 \text{ AM} - 6 \text{ PM} & (\text{light on}) \\ d & 6 \text{ PM} - 6 \text{ AM} & (\text{light off}) \end{cases} \quad (2)$$

in which d is a positive constant, introduces a forcing term in an otherwise autonomous system. The function $g(t)$ has been chosen so that $g(t) > 0$ (and so raises B_1) during the night, when activity is higher, and $g(t) = 0$ during the day. We find that the forced system also has a stable periodic

A Pharmacodynamic Turnover Model

orbit which attracts orbits starting at arbitrary initial values. It has the same period as the Timekeeper.

The generic function B_1 then needs to be rescaled to the size of the actual physiological variable (e.g., body temperature, blood pressure or heart rate) and its corresponding *amplitude* (Block 3 Fig. 1, reference temperature T_{ref} (e.g., 37.3 °C for body temperature) and *amplitude* (e.g., 3% for body temperature). The *amplitude* parameter reflects the peak-to-trough difference in e.g., body temperature. However, direct translation of the final estimate of the *amplitude* parameter to the observed absolute peak-to-trough difference is slightly confounded by the asymmetric behaviour of B_1 . This new function, T_{baseline} is then

$$T_{\text{baseline}} = T_{\text{ref}} \cdot (1 + \text{amplitude} \cdot B_1) \quad (3)$$

The observed baseline temperature (blood pressure, heart rate) is therefore a combination of B_1 , $g(t)$, T_{ref} and the *amplitude*. The mathematical behaviour of the baseline model and an introduction to the phase-plane plots are given in Appendix A.

Modelling of Hypothermia

The acute hypothermic effect of the test compound was modelled by means of a stimulatory function, S_1 , acting on the loss of response

$$\frac{dT}{dt} = k_{\text{in}} - k_{\text{out}} \cdot (1 + S_1) \cdot T \quad (4)$$

where k_{in} and k_{out} are turnover rate and fractional turnover rate constants, respectively, and T represents the hypothermic response uncorrected for animal-handling (Block 4, Fig. 1). The stimulatory function of the test compound, S_1 , was a sigmoid function:

$$S_1 = \frac{S_{\text{max}1} \cdot C^n}{\text{SC}_{50}^n + C^n} \quad (5)$$

where C is the (population) mean plasma exposure to the test compound, $S_{\text{max}1}$ is the maximum test compound-induced stimulus and SC_{50} is the concentration giving 50% of $S_{\text{max}1}$. The n parameter represents the sigmoidicity factor influencing the steepness of S_1 at SC_{50} . When no test compound is present, the hypothermic response T becomes

$$T_0 = \frac{k_{\text{in}}}{k_{\text{out}}} = T_{\text{ref}} \quad (6)$$

This expression can then be rearranged to give the turnover rate k_{in}

$$k_{in} = k_{out} \cdot T_{ref} \quad (7)$$

The steady-state response at constant exposure to the test compound is given by

$$T_{ss} = \frac{k_{in}}{k_{out}} \cdot \frac{1}{(1 + S_1)} \quad (8)$$

T_{ss} will then approach $(k_{in}/k_{out} \cdot 1/(1 + S_{max1}))$ when exposure to the test compound C , is much greater than SC_{50} .

Modelling of Tolerance Development

In light of the presented experimental setting and observed data pattern, there was not enough support to also include a homeostatic temperature controller. We therefore applied a model with a primary hypothermic effect with a parallel independent action on a tolerance function Q of the test compound. The impact of tolerance, Q , was modelled as desensitisation to the induced hypothermia. Since no rebound effects were seen after removal of the Alzet[®] pump, we have chosen a simple turnover model governing tolerance Q . Tolerance development was assumed to be triggered by the plasma exposure to the test compound, and not *via* the actual temperature decrease *per se* (Block 5, Fig. 1). The test compound stimulates the loss of Q *via* the drug ‘mechanism function’ S_2 , as shown in Eq. (9)

$$\frac{dQ}{dt} = k_{tol,in} - k_{tol,out} \cdot (1 + S_2) \cdot Q \quad (9)$$

where $k_{tol,in}$ and $k_{tol,out}$ are zero- and first-order rate constants, respectively. The induced stimulus, S_2 , is defined as

$$S_2 = \frac{S_{max2} \cdot C}{SC_{50} + C} \quad (10)$$

having a similar potency, SC_{50} , but a separate maximum level, S_{max2} , compared to the stimulus driving the hypothermia (Eq. (5)). In the absence of the test compound, Q_0 is set to unity according to

$$Q_0 = \frac{k_{tol,in}}{k_{tol,out}} = 1 \quad (11)$$

A Pharmacodynamic Turnover Model

In the presence of the test compound, Q_{ss} is written as

$$Q_{ss} = \frac{1}{1 + S_2} \quad (12)$$

Q_{ss} will then approach $1/(1 + S_{\max 2})$ when exposure to test compound C is much greater than SC_{50} .

Modelling of Animal-handling

The handling of animals during surgery or oral gavage caused a transient increase in body temperature due to the trauma independently of the pharmacological action of the test compound or vehicle (Block 6, Fig. 3). This handling effect, HD, was modelled as an exponential function with intensity and rate of dissipation by means of

$$HD = P \cdot e^{-k_{HD} \cdot (t - t_{HD})} \quad (13)$$

for $t > T_{HD}$. An alternative approach, however not applied in this study, is using a first-order onset/offset of the handling effect by means of Eq. (14).

$$HD = k_{HD} \cdot P \cdot (t - t_{HD}) \cdot e^{-k_{HD} \cdot (t - t_{HD})} \quad (14)$$

where t_{HD} is the time-point of animal-handling, P determines the magnitude of the temperature elevation and k_{HD} is the first-order loss of impact of handling.

The handling function was then incorporated into the hypothermic turnover model (Eq. (4)) as a stimulatory action of the turnover rate, k_{in} , giving

$$\frac{dT}{dt} = k_{in} \cdot (1 + HD) - k_{out} \cdot (1 + S_1) \cdot T \quad (15)$$

Modelling of the Integrated Temperature Model

The integrated temperature model TEMP (Eq. (16)) consists of seven basic parts (Blocks 1–7 in Fig. 1), namely, the free-running baseline model (Eq. (1)), correction for reference point T_{ref} and *amplitude* (Eq. (3)), the hypothermic model (Eq. (4)), the tolerance model (Eq. (9)), the animal-handling model (Eq. (13)) and exposure to test compound. Equation (16)

was then regressed to response–time data (body temperature) collected from the subcutaneous infusions of the test compound.

$$\text{TEMP} = T_{\text{baseline}} + (T - T_{\text{ref}}) \cdot Q \quad (16)$$

The steady state condition of TEMP at constant drug exposure is given by Eq. (17), by combining Eqs. (4, 5 and 8) with Eq. (16).

$$\text{TEMP}_{\text{ss}} = T_{\text{baseline}} - \frac{S_{\text{max}1} \cdot T_{\text{ref}}}{1 + S_{\text{max}1}} \cdot \frac{1}{1 + S_{\text{max}2}} \quad (17)$$

which may be used to evaluate different exposure patterns to the test compound. Note that HD does not contribute to TEMP at steady state because of its transient behaviour.

Data Pruning, Initial Parameter Estimates and Modelling

All datasets were rigorously explored prior to clean file. Sudden external stimuli such as noise or vibration may produce periods of transient changes in the body temperature measurements beyond the natural variability when animals are resting. Consequently, spurious spikes in the observed response–time profiles due to transmission errors, blood sampling procedures or environmental factors were removed. A standardised response–time profile of body temperature was constructed by averaging data from six control animals. For analysis of heart rate and blood pressure baselines, mean 96 hr profiles from 10 animals were used.

Initial estimates of T_{ref} , *amplitude*, k_{out} , $k_{\text{out,tol}}$ and $S_{\text{max}2}$ were derived graphically, and estimates of α , β and $g(t)$ were obtained from a *free-running* dataset ($g(t) = 0$). Literature data of Lobo *et al.* (6) served as a training dataset for deriving initial estimates of α and β in an individual rat exposed to constant darkness.

WinNonlin was used for regression of mean baseline data (α , β and $g(t)$, Lobo *et al.* (6)). These parameters were then treated as fixed values in the regression of the integrated model to individual animal temperature profiles by means of NONMEM (7). NONMEM software version V, Level 1.1 (University of San Francisco) was used, running on a Linux platform. The conditional estimation method was used in estimation of the population parameters. Model discrimination was based on goodness of fit plots, simulations and changes in NONMEM's objective function value. The evaluation of goodness-of-fit was performed by means of the weighted residual sum of squares and residual plots in WinNonlin (8).

A Pharmacodynamic Turnover Model

The integrated model was then challenged by using the regressed parameters for model simulations of repeated oral dosing. Model simulations and sensitivity analyses were done in Berkeley Madonna (9) and NONMEM.

RESULTS

Exposure to Test Compound

The PK for oral and continuous s.c. administration was obtained from satellite animals. Therefore, the population estimates were used for the simulation of the plasma concentrations during the pharmacodynamic experiment. Each animal was assumed to have the same plasma profile in each dose group. The exposure to the test compound was described by a first-order input/output kinetic model for individual data and was then treated as fixed for the subsequent pharmacodynamic modelling. Observed and model-predicted concentration-time courses of the test compound are shown in Fig. 2. The population PK parameter estimates (Table II) were used to calculate population exposure profiles. Because satellite animals were used, no individual exposure could be used.

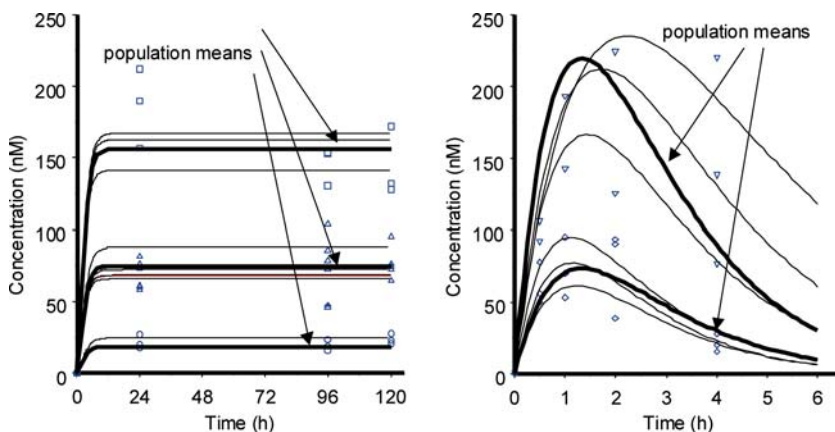


Fig. 2. Linear plasma concentration–time plots for test compound after continuous s.c. infusions for 5 days (left) of 25 (circles, 20 nm steady-state concentration), 100 (triangles, 75 nm steady-state concentration) and 200 $\text{nmol}\cdot\text{kg}^{-1}\cdot\text{h}^{-1}$ (squares, 150 nm steady-state concentration) and a single oral dose day 7 (right) of 250 (diamonds) and 750 (triangles) $\text{nmol}\cdot\text{kg}^{-1}$. Markers denote individual observed values, thin lines denote fitted individual functions and bold lines the population means.

Table II. Parameters, Population Estimates, Precision, and Interindividual Variability using NONMEM, and Routes for the One-compartment Pharmacokinetic Model Fitted to the Test Compound Plasma Concentration Data

Parameter	Unit	Estimate	SE%	CV%
Cl	L · kg ⁻¹ · min ⁻¹	0.013	11	20
V	L · kg ⁻¹	1.2	3	_b
F _{sc}	–	0.7	12	_b
K _{a,sc}	min ⁻¹	0.012	67	_b
F _{po1}	–	0.58	11	_b
F _{po2}	–	1 ^a	–	_b
K _{apo}	min ⁻¹	0.014	12	39

Cl = clearance, V = volume, F_{sc} = s.c. bioavailability, K_{a,sc} = s.c. absorption rate constant, F_{1,po} = p.o. bioavailability (400 nmol/kg dose experiment), F_{2,po} = p.o. bioavailability (250 and 750 nmol/kg doses experiment), K_{a,po} = p.o. absorption rate constant, CV = coefficient of variation.

^aFixed at 1.

^bFixed at zero. F was estimated from intravenous data not shown here.

Modelling of the Circadian Rhythm

The model adequately described the asymmetric light on/off temperature profile, with a low (~37.2 °C) but slowly increasing temperature during light on, an abrupt increase when the light was turned off, a relatively constant temperature (~37.8 °C) when the light is off and a rapid fall when the light was turned on again (Fig. 3). Rapid ultradian oscillations for both light on and light off appeared to occur in a random manner and were therefore not modelled as a part of the circadian clock.

The observed and model-predicted biorhythms of blood pressure and heart rate in control animals were consistent (Fig. 4, Table III), demonstrating the generic properties of the model. The typically asymmetric diurnal shape, amplitude and cycle-time were captured by the model.

A comparison of estimated parameter values obtained by fitting the system of equations Eq. (1) to the response profiles of body temperature, blood pressure and heart rate are shown in Table III.

The estimates of α (0.026 min⁻¹) and β (0.0037 min⁻¹) are consistent with scanned and analysed temperature data in the literature of α (0.04 min⁻¹) and β (0.002 min⁻¹) from an individual rat (6). These data also displayed an *amplitude* of 0.06 and a reference temperature T_{ref} of 37.5 °C. The impact on response of going from daylight to darkness (d) was consistent across responses (d was approximately 0.05 for body temperature, 0.04 for blood pressure and 0.04 for heart rate). The scaling parameters T_{ref} and *amplitude* are typically response-dependent. The

A Pharmacodynamic Turnover Model

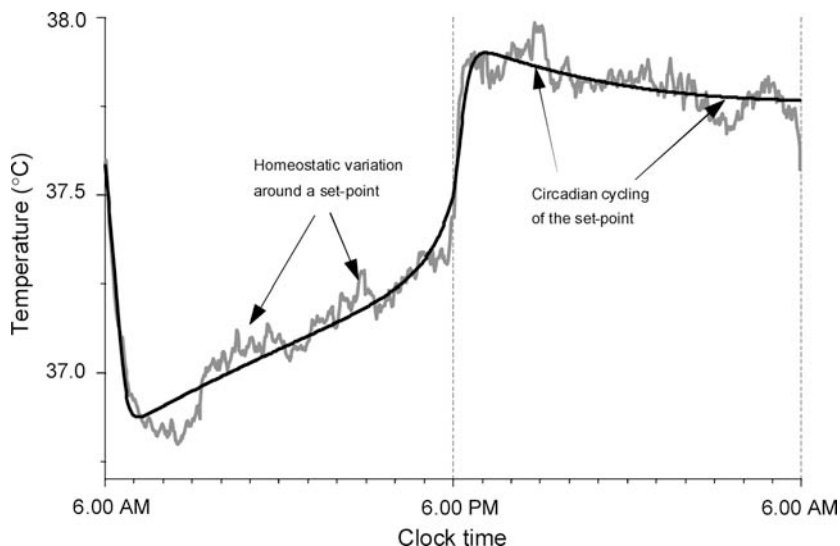


Fig. 3. Schematic illustration depicting the homeostatic and circadian variations in body temperature. Body temperature is constantly fluctuating at any moment as negative feedback (homeostasis) attempts to maintain the temperature at a set point. The set point itself cycles over a 24-hr period. Circadian rhythm of body temperature in untreated rats with a 12:12 hr light–dark cycle. The observed 24 hr temperature profile (jagged curve) was constructed by averaging data collected during a 9-day period. The model (smooth line) describes the shape, amplitude and period of experimental data. The horizontal white/black bar represents the external 12:12 hr light/dark cycle. Nomenclature according to Foster and Kreitzman (2).

amplitude estimates show 3, 10 and 40% changes around the T_{ref} values for body temperature, blood pressure and heart rate, respectively.

Simulations performed with the baseline model (Eqs. (1) and (3)) and the final parameter estimates of α and β , T_{ref} and *amplitude* in Table III revealed a free-running biorhythm in the absence of the Timekeeper, i.e. when $g(t)$ was set to zero (Fig. 5). The response–time course of the system was then symmetric, had lower amplitude, shorter period, and less pronounced temperature shifts.

Modelling Tolerance Development

Tolerance Development During Extended Exposure to Test Compound

The integrated model was regressed to individual body temperature data of 12 rats exposed to the steady-state test compound condition established from continuous s.c. infusions for 5 days. The observed and model-predicted response–time data were consistent at all dose levels (Fig. 6).

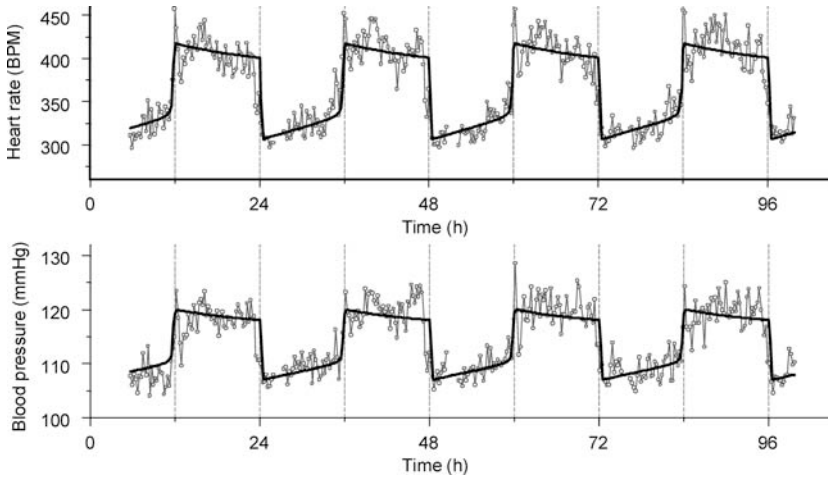


Fig. 4. Circadian baseline rhythm of blood pressure (bottom plot) and heart rate (upper plot) in control animals with a 12:12-hr light/dark cycle. The observed 96 hr response profiles (circles) were constructed by averaging data from 10 control animals. The model (solid line) describes the shape, amplitude and period of experimental data. The horizontal white/black bar represents the external 12:12 hr light/dark cycle. Parameter settings according to Table III.

Table III. Parameters, Units, Estimates and Relative Standard Deviations (CV%, Interindividual Variability using WinNonlin) of Body Temperature, Blood Pressure, and Heart Rate in Control Animals

Parameter	Body temperature			Blood pressure			Heart rate		
	Unit	Estimate	CV%	Unit	Estimate	CV%	Unit	Estimate	CV%
α	min^{-1}	0.026	5	min^{-1}	0.20	5	min^{-1}	0.092	20
β	min^{-1}	0.0037	3	min^{-1}	0.0018	1	min^{-1}	0.0022	5
d	–	0.053	2	–	0.042	3	–	0.036	10
T_{ref}	$^{\circ}\text{C}$	37.3	0.02	mmHg	113	0.1	bpm	357	0.5
amplitude	–	0.033	2	–	0.10	3	–	0.37	10

As shown in Fig. 6 complete tolerance to the hypothermic effect developed within 8–24 hr, in spite of a systemic exposure of 20, 75 and 150 nm to test compound. The variability in data seemed to increase with increasing exposure to test the compound over the experimental period. The final population parameter estimates obtained by regressing the integrated model (Eq. (16)) to experimental data from the 5-day continuous

A Pharmacodynamic Turnover Model

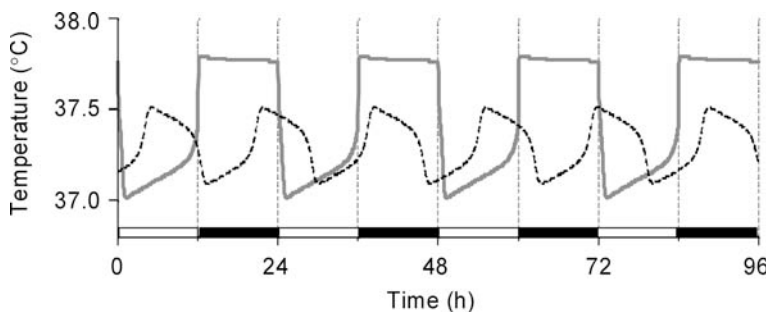


Fig. 5. Simulation of the biorhythm model in the absence of an external light/dark cycle (dotted symmetric line) showed stable oscillations with a shorter period and lower amplitude compared to when the light/dark cycle was present (solid asymmetric line). Parameter values are taken from Table III.

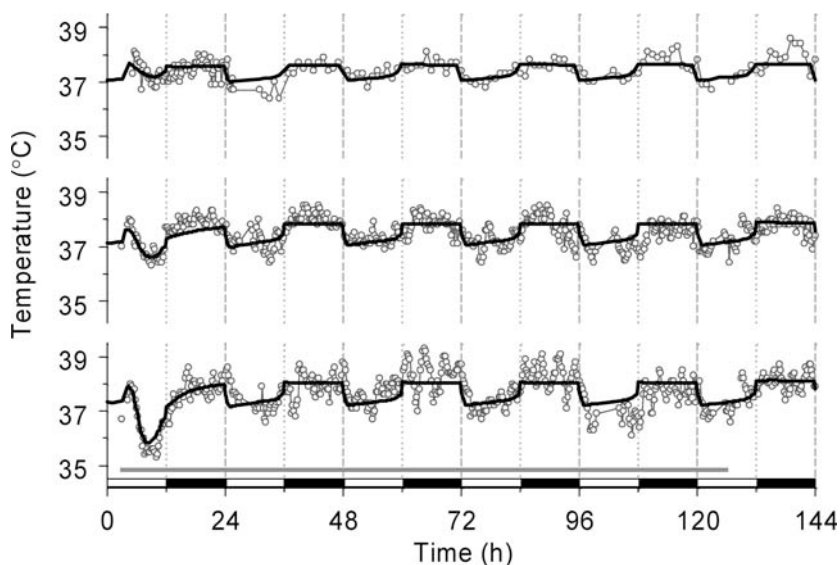


Fig. 6. Observed and model-predicted temperature data in three individual rats at 25, 100 and 200 $\text{nmol} \cdot \text{kg}^{-1} \cdot \text{h}^{-1}$ for five consecutive days. The solid light bar represents the length of exposure to test the compound. Note that complete tolerance is developed within 12–24 hr in spite of exposure to test compound, and the absence of rebound upon cessation of the s.c. infusion on day 5. The white/black bar represents the light/dark cycle. Parameter settings according to Table III. Systemic exposures were 20, 75, and 150 nm at the 25, 100 and 200 $\text{nmol} \cdot \text{kg}^{-1} \cdot \text{h}^{-1}$ doses, respectively, for five consecutive days.

Table IV. Parameters, Units, Estimates and Relative Standard Deviations (CV%, Inter-individual Variability using NONMEM) of the Integrated Temperature Model (Eq. (15)) in Animals Exposed the Test Compound

Parameter	Unit	Estimate	CV%
$S_{\max 1}$	–	0.2*	–
SC_{50}	nM	137	11
n	–	2*	–
k_{out}	min^{-1}	0.026	31
$S_{\max 2}$	–	74	81
$k_{\text{out, tol}}$	min^{-1}	$9.5 \cdot 10^{-5}$	74
P	–	0.017	31
k_{HD}	min^{-1}	0.01*	–
T_{ref}	$^{\circ}\text{C}$	37.8	0.1

*Fixed values.

infusion are shown in Table IV. The intra-individual variability was 18% for the pharmacokinetics.

Since tolerance development-confounded assessment of the maximum test compound induced a decrease in body temperature, the $S_{\max 1}$ parameter was fixed at 0.2, corresponding to a body temperature reduction to 31°C . The potency, SC_{50} , was estimated at $137 \text{ nm} \pm 11\%$ and the response half-life was about $30 \text{ min} \pm 31\%$. The sigmoidicity parameter n was fixed at 2 due to its high correlation with other parameters. The handling effect of vehicle-treated animals had a half-life of about 70 min, which was fixed. The estimated maximum stimulation of loss of tolerance, $S_{\max 2}$, of $74 \pm 81\%$ corresponds to a maximum tolerance development of about 98% (Eq. (12)). The half-life of the induced tolerance was about 5 days, predicting that tolerance effects can persist long after test compound ($t_{1/2} 60 \text{ min}$ in plasma) has been eliminated from the body.

Inserting the final parameter estimates of T_{ref} , $S_{\max 1}$ and $S_{\max 2}$ into Eq. (17) gives a reduction in body temperature of about 0.2% at steady-state. This minute decrease is due to the extensive tolerance development to test compound-induced hypothermia.

Simulations: Impact of Repeated Oral Administration

The integrated model was then simulated using an oral (gavage) input function combined with the final parameter estimates in Table IV. No interindividual variability was estimated for the drug parameters, only for the baseline (<1%) and amplitude (18%), in order to accommodate for the individual variability. Intraindividual variability for the pharmacodynamics was 1%.

A Pharmacodynamic Turnover Model

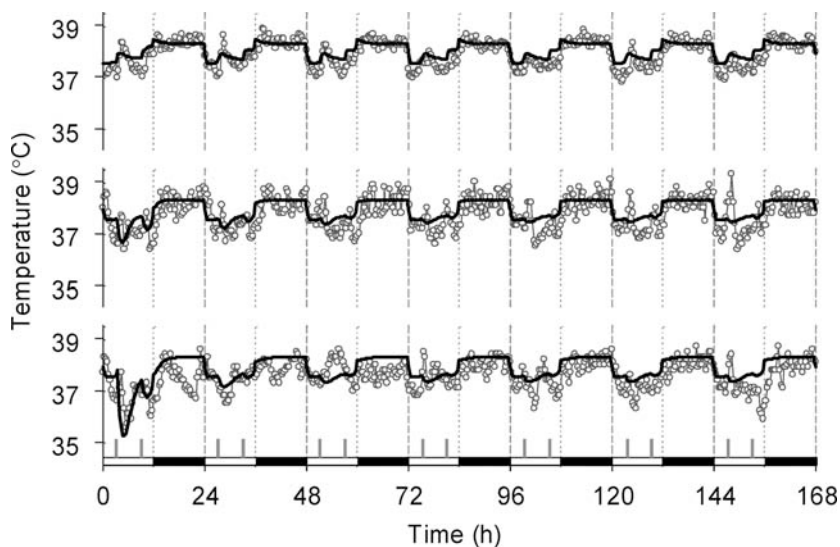


Fig. 7. Observed and model-simulated temperature data in three individual rats at 0, 500 and 1500 $\text{nmol} \cdot \text{kg}^{-1} \cdot \text{day}^{-1}$ during seven days of oral dosing (gavage). The vertical light bars represent the dosing times of the test compound. Note the absence of rebound between the doses. The white/black bar represents the light/dark cycle. Parameter settings according to Table III.

The simulation was performed with the population estimates assuming no inter-individual variability, thus simulating the population prediction of temperature response to repeated oral dosing. Superimposed experimental and model-predicted data are shown in Fig. 7 for 0,500 and 1500 nmol/kg/day of the test compound.

DISCUSSION

Body Temperature Regulation

Preclinical studies of drug effects on body temperature regulation and cardiovascular function such as heart rate and blood pressure are part of the required “core battery studies” (ICH S7A guidelines) performed before first-time administration in humans. Telemetric systems allow continuous high-resolution measurements in freely moving animals over extended periods of time under varying experimental conditions. This is advantageous since no animal-handling with respect to collection of data is needed that might compromise the interpretation of measured response (10).

At any moment, body temperature is oscillating rapidly about a *set point* as these negative feedback mechanisms attempt to maintain the set

point. However, the set point itself varies over a 24-hr period, falling at night and rising during the day (2). In contrast to this view, studies in rats (11,12) and humans (13) suggest that the fluctuations in body temperature caused by the normal circadian rhythm reflect internally forced deviations from the set point, rather than changes in the set point itself. In addition, some drugs are thought to change the setpoint.

Temperature regulation in the rat is controlled *via* the anterior hypothalamus with serotonin as an important mediator of the maintenance of the setpoint (14,15). In order to characterise 5-HT_{1A}-agonist-induced hypothermia in rats, Zuideveld *et al.* applied a turnover model with fixed baseline and set point values (16). Their model was partly based on the Ackerman *et al.* (17) negative feedback model and partly on drug-induced regulation of a set point parameter (thermostat).

Modelling of the Circadian Baseline

In this analysis, a novel pharmacodynamic model was developed for the circadian oscillations in body temperature. The concepts of feedback regulation originates from the work by Ackerman *et al.* (17) who originally developed a homeostatic glucose–insulin model. However, unlike a homeostatic system, which is always attempting to return to and stay at a fixed point, a self-sustained oscillator like a circadian clock tends to move away in a regular manner from one state to another. The system developed in this paper, can describe the basic features of the body temperature profiles seen in untreated and vehicle-treated animals, including asymmetric light on/off profiles and entrainment by an external timekeeper $g(t)$. The estimates of $\alpha(0.026 \text{ min}^{-1})$ and $\beta(0.0037 \text{ min}^{-1})$ are consistent with scanned and analysed temperature data in the literature of $\alpha(0.04 \text{ min}^{-1})$ and $\beta(0.002 \text{ min}^{-1})$ from an individual rat (6). These data also displayed an *amplitude* of 0.06 and a reference temperature (T_{ref}) of 37.5 °C. The transition time ($\approx 2/\alpha$) was over an hour (80 min) for body temperature compared to 10–20 min for blood pressure (10 min) and heart rate (22 min). This seems logical since a change in body temperature is a consequence of a change in energy consumption due to changes in blood pressure and heart rate. The proposed model fulfils a number of basic conditions set up for biorhythm models: (a) stable oscillations in the absence of an external timekeeper $g(t)$, (b) adaptation of the phase and period when the timekeeper $g(t)$ is introduced, and (c) preservation of phase but not period, when the light on/off-cycle is removed (1,2). Moreover, analyses of heart rate and blood pressure in the conducted experiments have revealed similar circadian profiles to those for body temperature, making the proposed model applicable to other physiological effects besides body temperature.

A Pharmacodynamic Turnover Model

The model predicts qualitatively different behaviour under constant light vs. constant dark conditions. Indeed, constant light and constant dark conditions have been reported to cause different temperature patterns in rats (18). These experiments show stable oscillations under constant dark conditions and suppressed oscillations under constant light conditions. The proposed model predicts stable oscillations under constant light conditions and no oscillations under constant dark conditions. The goals for the next generation of models are to capture such behaviour.

Trigonometric models have previously been reported to work well for circadian rhythms in rats and humans (4). For lower organisms such as *Drosophila* and *Neurospora*, the molecular basis is better understood. A bottom-up approach has been adopted, allowing a mechanistic analysis (19,20). Moreover, homologues of many of the genes found in the circadian clock in lower organisms have been found in mammals (21), and preliminary molecular descriptions of the mammalian system have been proposed (22,23, for review see Foster and Kreitzman (2)). These models feature negative feedback similar to what is proposed here by means of a top-down analysis based on functional responses.

Hypothermia and Tolerance Development

Hypothermia induced by the test compound was described with a standard turnover model where the test compound acts *via* stimulation of loss. If no tolerance is present, the model predicts a maximum temperature decrease of about 6.5 °C, resulting in a body temperature of about 31 °C.

Complete tolerance development was observed within the first 12–24 h during constant exposure to the test compound for 5 days (Figs. 2 left and 6). This is particularly clear for the high constant exposure group (Fig. 6). In spite of this, no rebound effect was seen on withdrawal of the test compound. Alternative models, such as the precursor or basic feedback models showed rebound effect and were therefore not appropriate (24–28). Instead, tolerance was modelled with Eq. (9), thereby avoiding any rebound effect. Moreover, tolerance was assumed to depend indirectly on exposure to the test compound rather than on the induced hypothermia.

Our subjective impression is that the variability in data seemed to increase with increasing exposure to the test compound over the experimental period of 5–7 days as compared to vehicle control animals. This is an observation that we have also seen for drugs such as clomethiazole and for which we do not have an explanation (29).

The final step in the modelling carousel is to make “what-if?” predictions. The purpose of this may be experimental design or assessing exposure-response risk. The strength of the integrated temperature model was

demonstrated by means of model simulations for oral administration (gavage) of the test compound. We have therefore considered a separate experiment, not part of the regression analysis, as a “validation dataset”. Model-predicted and experimental data were surprisingly consistent. One may argue that the model systematically over- or underpredicted the 3–5 nighttime response patterns. One reason for the deviation is that no baseline measurements were done in drug free animals used for this comparison, making it impossible to correct for the individual baseline amplitude. However, the deviation was in general less than 0.5 °C. In light of adequately capturing the four pharmacodynamic complexities, such as asymmetric biorhythm, drug effects, tolerance and animal-handling effects, the model has a strong potential for “what-if” predictions and experimental design.

An appropriate treatment of pharmacodynamic complexities such as the asymmetric baseline, tolerance, handling effect etc. is critical for characterisation of the pharmacodynamic properties of a compound, assessment of safety margin and prediction of clinical doses. Setting the baseline to a constant value or subtracting baseline or vehicle-treated groups from the treatment-response-time course are commonly done, but is, nevertheless, prone to imprecise and biased interpretation.

In conclusion, a new mathematical model was developed for the prediction of asymmetric baseline oscillations in body temperature, heart rate and blood pressure. The model was extended to incorporate handling effects and tolerance to body temperature caused by extended constant exposure to the test compound. Simulations of the integrated temperature model succeeded in mimicking other modes of administration such as oral dosing.

ACKNOWLEDGMENTS

We would like to thank Kristina Tällö and Sylvia Ekstrand, who were responsible for collection of *in vivo* data.

APPENDIX A

The Free-running Biorhythm Model

The free-running biorhythm model does not contain any time-dependent light/dark function and is thus given by

$$\begin{cases} \frac{dB_1}{dt} = \alpha \cdot (B_1 - B_2) - B_1^3 \\ \frac{dB_2}{dt} = \beta \cdot (B_1 - B_2) \end{cases} \quad (\text{A:1})$$

A Pharmacodynamic Turnover Model

where B_1 is assigned to be the component of the free-running rhythm and B_2 an associated complimentary variable. This is an autonomous system of differential equations, since the right-hand sides of equation (A:1) do not contain time explicitly. See also Kaplan and Glass (28) for a description of the classical Van der Pol oscillator.

Phase-plane Analysis

In the phase plane analysis of the system (A:1), solutions are represented as orbits in the (B_1, B_2) -plane. The velocity vector (B'_1, B'_2) , where primes denote differentiation with respect to t , is then given by the right-hand sides of the system (A:1). Of particular importance are the nullclines along which the vector field is either vertical ($B'_1 = 0$) or horizontal ($B'_2 = 0$). We denote the first nullcline by Γ_1 and the second nullcline by Γ_2 . From the system of equations (A:1) we deduce that they are given by

$$\begin{aligned}\Gamma_1 : B_2 &= h_1(B_1) =: B_1 - \frac{1}{\alpha} \cdot B_1^3 \\ \Gamma_2 : B_2 &= h_2(B_1) =: B_1\end{aligned}$$

Stationary points, where $B'_1 = 0$ as well as $B'_2 = 0$, are points where Γ_1 and Γ_2 intersect. In this problem the only stationary point is the origin $(B_1, B_2) = (0, 0)$. In Fig. A.1 (left), the phase plane of Eq. (A:1) is shown with the nullclines and an orbit. Arrows denote directions of the velocity vector field as given by the right-hand side of Eq. (A:1).

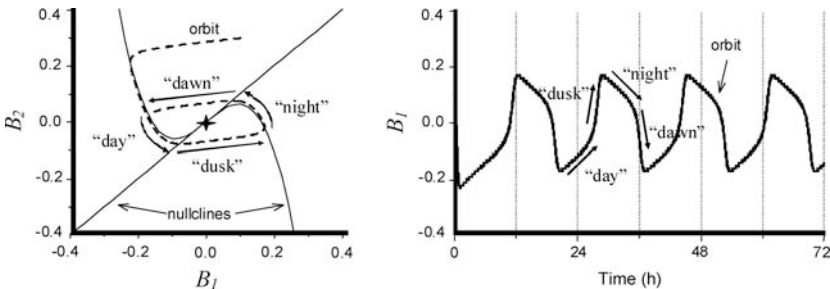


Fig. A.1. The oscillations of the biorhythm in its free-running state shown in the phase plane (left) and in the baseline-time plot (right). Based on the shape of the curve, every cycle is divided into four periods named according to observed data for which a light/dark cycle is present. Parameter settings according to Table III where α is 0.026 min^{-1} and β 0.0037 min^{-1} . Nullcline: A curve in the (B_1, B_2) -plane on which the vector field is either horizontal ($dB_1/dt = 0$), or vertical ($dB_2/dt = 0$). A Solution to the system: $B_1(t)$ and $B_2(t)$ can be viewed as a curve(orbit) in the phase plane.

It can be shown that if $\alpha > \beta$, then there exists a stable periodic orbit as shown in Fig. A.1 (right). This orbit serves as an attractor of orbits starting at arbitrary points in the phase plane, away from the origin.

Initial Estimates of Parameters

It is evident from the equations (A:1) that the parameter α affects the rate of change of B_1 and that β affects the rate of change of B_2 . Thus, to account for the rapid transitions of B_1 , we need to take α much larger than β . We define the duration of a “night” as *NightTime* and the duration of a transition period as *TransitionTime*. Reasonable initial estimates of the parameters α and β are then given by

$$\begin{aligned} \alpha &\approx \frac{2}{\text{TransitionTime}} \\ \beta &\approx \frac{2}{\text{NightTime}} \end{aligned} \quad (\text{A:2})$$

where *NightTime* and *TransitionTime* are obtained by visual inspection of the observed data.

In the present paper, data were only available from experiments with a light/dark cycle present. *TransitionTime* and *NightTime* in the observed data can thus be expected to differ somewhat from the free-running system and approximate values must be chosen.

The Biorhythm Model with a Light/Dark Cycle

The biorhythm system with the light/dark cycle is defined as

$$\begin{cases} \frac{dB_1}{dt} = \alpha \cdot (B_1 - B_2) - B_1^3 + g(t) \\ \frac{dB_2}{dt} = \beta \cdot (B_1 - B_2) \end{cases} \quad (\text{A:1})$$

where

$$g(t) = \begin{cases} 0 & 6 \text{ AM} - 6 \text{ PM} \quad (\text{Day}) \\ d & 6 \text{ PM} - 6 \text{ AM} \quad (\text{Night}) \end{cases} \quad (\text{A:3})$$

and d is a real positive number. The nullcline Γ_1 is thus given by

$$\Gamma_1 = \begin{cases} B_1 - \frac{1}{\alpha} \cdot B_1^3 & 6 \text{ AM} - 6 \text{ PM} \quad (\text{Day}) \\ B_1 - \frac{1}{\alpha} \cdot B_1^3 + \frac{d}{\alpha} & 6 \text{ PM} - 6 \text{ AM} \quad (\text{Night}) \end{cases} \quad (\text{A:4})$$

A Pharmacodynamic Turnover Model

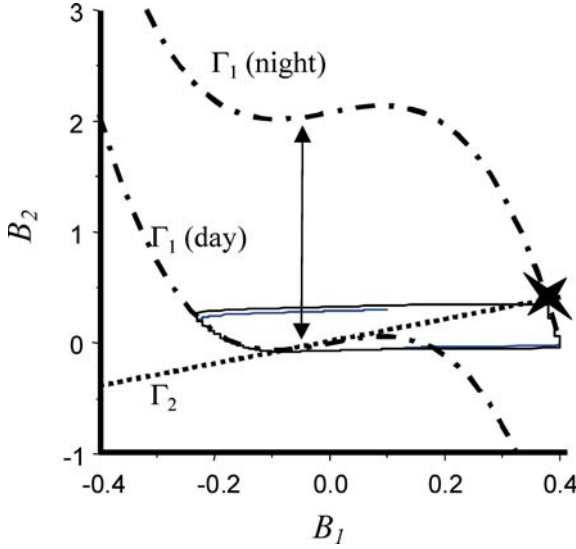


Fig. A.2. Phase plane of the biorhythm model in the presence of an external light/dark cycle (Timekeeper), with a trajectory (solid line) starting at $(B_1, B_2) = (0.1, 0.3)$. The arrow indicates the shift of the nullcline Γ_1 from its daytime position (dot-dash line) to its night-time position (dotted line). The nullcline Γ_2 and the fixed point during the night (star) are also shown. Note that the two axes have different scales. Parameter settings according to Table III where α is 0.026 min^{-1} and β 0.0037 min^{-1} .

During the night, the nullcline Γ_1 is thus shifted upwards (Fig. A.2) and the fixed point is moved to the new intersection of the two nullclines, given by

$$\begin{aligned} \Gamma_1(\text{Night}) = \Gamma_2 &\Leftrightarrow B_1 - \frac{1}{\alpha} \cdot B_1^3 + \frac{d}{\alpha} = B_1 \\ \Rightarrow B_1 &= \sqrt[3]{d} \end{aligned} \quad (\text{A:5})$$

and so the fixed point during the night is $(B_1, B_2) = (\sqrt[3]{d}, \sqrt[3]{d})$. For the values of α, β and d from Table III, the new fixed point is a stable node and during the night the orbit will tend to this point. At the start of the day, when Γ_1 is reset to its original level, the system will quickly approach the Γ_1 nullcline in the upper left area, and the oscillation will be resumed. Thus a periodic orbit is created which is stable and attracts orbits from a large set of initial data as the time tends to infinity. The nullcline transition causes the timing of the oscillation phase as well as the asymmetric day/night profile.

REFERENCES

1. M. Moore-Ede, F. Sulzman, and C. Fuller. *The Clocks that Time Us*. Harvard University Press, Cambridge, Massachusetts and London, England, 1982.
2. R. Foster and L. Kreitzman. *Rhythms of Life: The Biological Clocks that Control the Daily Lives of Every Living Thing*. Profile Books Ltd, London, Great Britain, 2004.
3. B. Lemmer. Chronopharmacokinetics: Implications for drug treatment. *J. Pharm. Pharmacol.* **51**:887–890 (1997).
4. A. Chakraborty, W. Krzyzanski, and W. J. Jusko. Mathematical modeling of circadian cortisol concentrations using indirect response models: Comparison of several methods. *J. Pharmacokinetic. Biopharm.* **27**:23–43 (1999).
5. D. Kaplan and L. Glass. *Understanding Nonlinear Dynamics*. Springer Verlag, New York, Berlin, Heidelberg, 1995.
6. L. L. Lobo, B. Claustrat, G. Debilly, L. Paut-Pagano, M. Jouvet, and J. L. Valatx. Hypoprolactinemic rats under conditions of constant darkness or constant light. Effects on the sleep-wake cycle, cerebral temperature and sulfatoxymelatonin levels. *Brain Res.* **835**:282–289 (1999).
7. A. Boeckman, L. B. Sheiner, and S. L. Beal. *NONMEM Users guide*, NONMEM project group, San Francisco, CA, University of California; 1992.
8. WinNonlin, www.Pharsight.com.
9. R. Macey and G. Oster. Berkeley Madonna, Modeling and analysis of dynamical systems. www.berkeleymadonna.com
10. R. Refinetti and M. Menaker. The circadian rhythm of body temperature. *Physiol Behav.* **51**:613–637 (1992).
11. E. Briesse. Rats prefer ambient temperatures out of phase with their body temperature circadian rhythm. *Brain Res.* **345**:389–393 (1985).
12. E. Briesse. Normal body temperature of rats: The set point controversy. *Neurosci. Biobehav. Rev.* **22**:427–436 (1998).
13. J. A. Shoemaker and R. Refinetti. Day-night difference in the preferred ambient temperature of human subjects. *Physiol Behav.* **59**:1001–1003 (1996).
14. J. Bligh. The central neurology of mammalian thermoregulation. *Neuroscience* **4**:1213–1216 (1979).
15. E. Zeisberger. Biogenic amines and thermoregulation changes. *Prog. Brain Res.* **115**:159–176 (1998).
16. K. P. Zuideveld, H. J. Maas, N. Treijtel, J. Hulshof, P. H. van der Graff, L. A. Peletier, and M. Danhof. A set-point model with oscillatory behaviour predicts the time course of 8-OH-DPAT-induced hypothermia. *Am. J. Physiol Regul. Integr. Comp Physiol.* **281**:R2059–R2071 (2001).
17. E. Ackerman, J. W. Rosevear, and W. F. McGuckin. A mathematical model of the glucose-tolerance test. *Phys. Med. Biol.* **9**:203–213 (1964).
18. P. Depres-Brummer, F. Levi, G. Metzger, and Y. Touitou. Light-induced suppression of the rat circadian system. *Am. J. Physiol.* **268**:R1111–R1116 (1995).
19. J. C. Leloup and A. Goldbeter. Modeling the molecular regulatory mechanism of circadian rhythms in *Drosophila*. *Bioessays* **22**:84–93 (2000).
20. P. Smolen, D. A. Baxter, and J. H. Byrne. Modeling circadian oscillations with interlocking positive and negative feedback loops. *J. Neurosci.* **21**:6644–6656 (2001).
21. M. W. Young and S. A. Kay. Time zones: a comparative genetics of circadian clocks. *Nat. Rev. Genet.* **2**:702–715 (2001).
22. L. P. Shearman, S. Sriram, D. R. Weaver, E. S. Maywood, I. Chaves, B. Zheng, K. Kume, C. C. Lee, G. T. van der Horst, M. H. Hastings, and S. M. Reppert. Interacting molecular loops in the mammalian circadian clock. *Science* **288**:1013–1019 (2000).
23. S. M. Reppert and D. R. Weaver. Coordination of circadian timing in mammals. *Nature* **418**:935–941 (2002).
24. E. B. Ekblad and V. Licko. Invariant relation between total acid secretion and secretagogue exposure: Secretory dynamics in bullfrog. *Am. J. Physiol. Gastrointest. Liver Physiol.* **246**: G325–G330 (1984).

A Pharmacodynamic Turnover Model

25. V. Licko and E. B. Ekblad. Dynamics of a metabolic system: what single-action agents reveal about acid secretion. *Am. J. Physiol. Gastrointest. Liver Physiol.* **262**: G581–G592 (1992).
26. J. A. Bauer and H. L. Fung. Pharmacodynamic models of nitroglycerin-induced hemodynamic tolerance in experimental heart failure. *Pharm. Res.* **11**:816–823 (1994).
27. J. Gabrielsson and D. Weiner. *Pharmacokinetic and Pharmacodynamic Data Analysis: Concepts and Applications*. 3rd edn, Swedish Pharmaceutical Press, Stockholm, Sweden; 2000.
28. E. A. Coddington and N. Levinson. *Theory of Ordinary Differential Equations*. McGraw-Hill, New York; 1955.
29. S. A. G. Visser, S. Pozarek, S. Martinsson, T. Forsberg, S. B. Ross, and J. Gabrielson. Rapid and longlasting tolerance to clomethiazole-induced hypothermia in the rat. *Eur. J. Pharmacol.* **512**:139–151 (2005).